

Title	The relationship between the fine structure of amylopectin and the 1 type of crystalline allomorph of starch granules in rice endosperm
Author(s)	Nakamura, Yasunori; Yashiro, Kazuki; Matsuba, Go; Wang, Yifei; Mizutani, Goro; Ono, Masami; Bao, Jinsong
Citation	Cereal Chemistry, 100(3): 721-733
Issue Date	2023-01-31
Type	Journal Article
Text version	author
URL	http://hdl.handle.net/10119/19680
Rights	This is the peer reviewed version of the following article: https://onlinelibrary.wiley.com/doi/full/10.1002/cche.10649 , which has been published in final form at https://doi.org/10.1002/cche.10649 . This article may be used for non-commercial purposes in accordance with Wiley Terms and Conditions for Use of Self-Archived Versions. This article may not be enhanced, enriched or otherwise transformed into a derivative work, without express permission from Wiley or by statutory rights under applicable legislation. Copyright notices must not be removed, obscured or modified. The article must be linked to Wiley's version of record on Wiley Online Library and any embedding, framing or otherwise making available the article or pages thereof by third parties from platforms, services and websites other than Wiley Online Library must be prohibited.
Description	



1 **The relationship between the fine structure of amylopectin and the**
2 **type of crystalline allomorph of starch granules in rice endosperm**

3
4
5 **Yasunori Nakamura^{a,b,*}, Kazuki Yashiro^c, Go Matsuba^c, Yifei Wang^d, Goro**
6 **Mizutani^d, Masami Ono^a, Jinsong Bao^e**

7
8 ^a *Starch Technologies Co., Ltd., Akita Prefectural University, Shimoshinjo-Nakano,*
9 *Akita-city, Akita 010-0195, Japan*

10 ^b *Faculty of Bioresource Sciences, Akita Prefectural University, Shimoshinjo-Nakano,*
11 *Akita-city, Akita 010-0195, Japan*

12 ^c *Graduate School of Organic Materials Engineering, Yamagata University, 4-3-16*
13 *Jonan, Yonezawa, Yamagata 992-8510, Japan*

14 ^d *School of Materials Science, Japan Advanced Institute of Science and Technology, 1-1*
15 *Asahidai, Nomi, Ishikawa 923-1292, Japan*

16 ^e *Institute of Nuclear Agricultural Sciences, Zhejiang University, Hangzhou 310058,*
17 *China*

18
19
20 *Corresponding author: Starch Technologies Co., Ltd., Akita Prefectural University,
21 Shimoshinjo-Nakano, Akita-city, Akita 010-0195, Japan.

22 E-mail address: nakayn@silver.plala.or.jp (Yasunori Nakamura)

37 **Abstract**

38

39 **Background and Objectives:** It is known that any wild-type varieties of cereals so far
40 examined have A-type starch crystals in their endosperm whereas their *starch branching enzyme*
41 *2b (be2b)* mutants that are usually referred to as *amylose-extender (ae)* mutants produce B-type
42 starch crystals. The present study aimed to examine the structural features of amylopectin which
43 are responsible for the A-type or B-type crystalline allomorphs of starch granules by using
44 starches in wild-type *japonica* and *indica* rice varieties and their *be2b (ae)* mutants.

45 **Findings:** The average length of chains of A-type amylopectin was markedly shorter than
46 that of B-type amylopectin. It was also thought that A-type amylopectin had two types of
47 branches, namely the first branches were formed mainly by BEI in the basal region of the
48 cluster and the second branches were synthesized specifically by BEIIb inside the cluster.
49 These differences caused the average length of double helices formed by cluster
50 constituent chains to be shorter in wild-types than that in their *be2b* mutants, and these
51 differences changed the crystalline allomorph of starch granules to B-type in the mutants
52 from A-type in their wild-types, as examined by wide angle X-ray diffraction (XRD) and
53 sum frequency generation spectroscopy (SFG).

54 **Conclusions:** Combined with these observations and calculations of chain-length of
55 hypothetical A chains in four types of amylopectin molecules, it was concluded that both
56 the average length of external segments of cluster chains and the formation of the second
57 branches inside the cluster greatly affect the crystal types of starch granules.

58 **Significance and Novelty:** The novel findings in the present study can provide new
59 insights into the structural features of amylopectin which determines the A-type or B-type
60 crystalline allomorph of starch granules of cereals.

61

62

63 **Keywords** A-type starch; B-type starch; rice endosperm; starch branching enzyme

64

65

66 **Abbreviations** *ae*, amylose extender; APTS, 8-amino-1,3,6-pyrenesulfonic acid; BE,
67 starch branching enzyme; DBE, starch debranching enzyme; DP, degree of
68 polymerization; FACE, fluorophore-assisted carbohydrate electrophoresis; Φ -LD,
69 phosphorylase-limit dextrans; PaISA, Isoamylase from *Pseudomonas amyloclavata*;
70 SFG, sum frequency generation spectroscopy; SS, starch synthase; XRD, wide angle X-
71 ray diffraction

72

73

74 **1 INTRODUCTION**

75

76 Rice plants have been widely used as materials for studies on starch biosynthesis. Rice
77 varieties are largely classified into *japonica*-type and *indica*-type varieties. Past
78 investigations have revealed that starch is synthesized by concerted actions of starch
79 synthase (SS), BE, and starch debranching enzyme (DBE). Although three starch
80 biosynthetic enzymes have multiple isozymes, their roles and expressions in various
81 organs and tissues are greatly different in rice plants (Ohdan et al., 2005). It has been
82 established that *japonica*-type rice is deficient in SSIIa, whereas *indica*-type rice has a
83 full activity of SSIIa (Umemoto et al., 2002; Nakamura et al., 2005).

84 Starch is composed of amylopectin, a highly branched glucan, and amylose, an
85 essentially linear glucan, and the amount of amylopectin usually accounts for 65-85% of
86 the total starch. Amylopectin is known to have a specific fine structure. This glucan has
87 a structural element called “cluster”, which is interconnected by long chains and aligned
88 basically in tandem fashion (French, 1972; Nakamura & Kainuma, 2022). Each cluster is
89 composed of A chains (non-branched chains) and B1 chains (branched by at least one
90 chains) and each cluster is interconnected by long chains designated as B2 chains and/or
91 B3/B4 chains that span to two/three clusters and/or three clusters, respectively (Peat et
92 al., 1952; Hizukuri, 1986). Very importantly, when non-branched segments of
93 neighboring chains of the cluster exceed 10 glucosyl units or degree of polymerization
94 (DP) of 10, they form double helices (Gidley & Bulpin, 1987). The presence of double
95 helices in amylopectin molecules dramatically affects physicochemical properties of
96 starch granules including amylopectin and amylose molecules. The clusters are packed
97 by the lateral alignment of neighboring double helices (Kainuma & French, 1972;
98 Yamaguchi et al., 1979; French, 1984). It is widely known that starch granules in cereal
99 endosperm show the A-type crystalline polymorph whereas some tubers and rhizomes
100 exhibit the B-type crystalline polymorph, which can be clearly distinguished by X-ray
101 diffraction analysis (see reviews by Hizukuri, 1996; Buléon et al., 1998). The A-type
102 starch is composed of a monoclinic unit cell whereas the B-type starch has a hexagonal
103 unit cell, and thus the A-type starch is considered to be more densely packed compared
104 with the B-type starch (see review by Imberty et al., 1991).

105 The phenotypes of BEIIb-deficient mutants of cereals are often designated as *ae* because
106 the *ae* mutant starches have apparently the high-amylose contents in the endosperm (see
107 review by Shannon et al., 2009). Interestingly, the *ae* starches in cereal endosperm show
108 the B-type crystalline allomorph (Gérard et al., 2000; Nishi et al., 2001; Tanaka et al.,

109 2004). The *be2b (ae)* mutants in *japonica*-type rice endosperm (Yano et al., 1985) have
110 a modified amylopectin chain profile because it contains more long B chains and fewer
111 short chains of $DP \leq ca. 13$ (Nishi et al., 2001; Nakamura et al., 2022). This change is
112 caused by loss of the distinct role of BEIIb, playing an essential role in the synthesis of
113 short chains in the region in the crystalline lamella of amylopectin cluster (Jane et al.,
114 1997; Nakamura et al., 2020). Based on these observations, recently we proposed that
115 amylopectin in endosperm of *japonica*-type rice and its *be2b* mutant is referred to as A-
116 type amylopectin and B-type amylopectin, respectively (Nakamura et al., 2022). On the
117 other hand, *indica*-type amylopectin has fewer short chains of $DP \leq 10$ and more
118 intermediate chains of $DP 12-24$ than *japonica*-type amylopectin whereas the proportion
119 of long chains is unchanged between these amylopectin (Umemoto et al., 1999;
120 Nakamura et al., 2002). However, *indica*-type starch granules exhibit A-type allomorph
121 as *japonica*-type starch granules (Hizukuri, 1996). In this sense, *indica*-type amylopectin
122 should be classified into an A-type amylopectin.

123 What is a criterion to distinguish the structural difference between A-type and B-type
124 amylopectin? In the present study, to analyze the structural difference between A-type
125 amylopectin and B-type amylopectin, the fine structure of endosperm amylopectin of
126 *be2b (ae)* mutants from both *japonica* rice and *indica* rice was analyzed in details, because
127 both *be2b* mutant starch granules would have B-type crystalline allomorph, whereas the
128 A-type amylopectin structure is known to be greatly different between *japonica* and
129 *indica* rice varieties. Therefore, these materials used in this study are extremely beneficial
130 to reveal the relationship between the fine structure of amylopectin and the crystalline
131 allomorph of starch granules. In addition, to analyze the internal structure of amylopectin,
132 chain-length distribution of its phosphorylase-limit dextrin (Φ -LD) was examined. To
133 reveal the relationship between the fine structure of amylopectin and the internal starch
134 structure of starch granule, starch crystalline structures were also examined using XRD
135 and SFG analysis (Miyachi et al., 2006; Kong et al., 2014).

136

137

138 2 MATERIALS AND METHODS

139

140 2.1 Reagents

141

142 A fluorophore 8-amino-1,3,6-pyrenesulfonic acid (APTS) was obtained from AB SCIEX
143 (Tokyo, Japan). α -Glucan phosphorylase from rabbit muscle was purchased from SIGMA.

144 Isoamylase from *Pseudomonas amyloideramosa* (PaISA) was kindly provided from
145 Hayashibara Co., Ltd., Japan.

146

147 **2.2 Plant materials and sampling**

148

149 Two *be2b* mutant lines EM10 and IR36*ae* were generated from a *japonica*-type cultivar
150 Kinmaze and an *indica*-type cultivar IR36, respectively. Mature seeds were also
151 harvested from each line which was grown in the experimental field of Akita Prefectural
152 University under natural environmental conditions during summer months, and stored at
153 8°C before use.

154

155 **2.3 Preparation of starch granules from rice endosperm**

156

157 Starch granules from randomly chosen mature endosperms of each line were prepared as
158 described previously (Nakamura et al., 2020).

159

160 **2.4 Chain-length distribution analysis of amylopectin**

161

162 The chain-length distribution of amylopectin was analyzed by using the fluorophore-
163 assisted carbohydrate electrophoresis (FACE) method (O'Shea et al., 1998) after
164 treatment of amylopectin with PaISA to remove α -1, 6-glucosidic linkages, followed by
165 labelling of APTS at the reducing ends of debranched glucan chains, as described
166 previously (Nakamura et al., 2020).

167

168 **2.5 Chain-length distribution analysis of phosphorylase-limit dextrins (Φ -LD) of 169 amylopectin**

170

171 Chain-length distribution of Φ -LD was analyzed to examine the internal structure of
172 amylopectin. In this analysis, amylopectin was treated with a rabbit muscle phosphorylase
173 to form its Φ -LD, as reported previously (Sawada et al., 2014). The Φ -LD was
174 debranched and its chain-length distribution was analyzed as above.

175

176 **2.6 X-ray diffraction (XRD) pattern analysis of starch granules**

177

178 XRD measurements were performed on a Nano-viewer system (Rigaku Co., Tokyo,
179 Japan) at a wavelength of 0.154 nm (CuK α). The camera lengths were 75 mm. A Pilatus

180 1M (Dectris AG, Baden, Switzerland) detector was used, with a q range of 3.5 to 25 nm⁻¹;
181 q is the magnitude of the scattering vector and is defined as follows:

$$182 \quad q = 4\pi \sin \theta / \lambda \quad (1),$$

183 where 2θ and λ are the scattering angle and wavelength, respectively. The starch granule
184 samples were put into the sample cell of approximately 500 μm thickness. Data
185 processing, which included controlling the contrast of the 2D-patterns and the preparation
186 of a 1D-profile from the obtained 2D-patterns, was performed using the FIT-2D software
187 (Ver. 12.077, Andy Hammersley/ESRF, Grenoble, France).

188

189 **2.7 Optical sum frequency generation (SFG) spectroscopy of starch granules**

190

191 The powdered starch samples of Kinmaze, IR36, EM10, and IR36*ae* were put in
192 transparent silica glass square cells (AS ONE Q-101; 3.5 mm \times 12.5 mm \times 45 mm). The
193 internal sizes of the cells were 1 mm in thickness and 10 mm in width. SFG of our sample
194 was observed through the glass window of the cell. The SFG spectroscopy system was
195 the same as previously described (Hieu et al., 2015; Nakamura et al., 2020). Tunable
196 infrared light pulses at wavelength of approximately 3 μm was output from an optical
197 parametric generator (EKSPLA PG401/DFG2-18P) pumped by the fundamental and third
198 harmonic output of a Nd³⁺:YAG laser (EKAPLA PL2143B) with time width 30 ps and
199 repetition rate of 10 Hz. The pulse energy of the visible light was about 10 μJ and that of
200 the infrared was about 260 μJ at the sample. The spectral width of the IR light was 6 cm⁻¹
201 ¹. For more details see our previous paper (Nakamura et al., 2020).

202

203

204 **3 RESULTS**

205

206 **3.1 Comparison of chain-length distribution of amylopectin in mature endosperm of** 207 ***be2b* mutant lines and their parent cultivars of *japonica*-type rice and *indica*-type** 208 **rice**

209

210 It is widely known that starch granules including amylopectin in mature endosperm of
211 wild-type rice from both *japonica*-type and *indica*-type varieties have the A-type
212 crystalline allomorph. We previously proposed that the rice amylopectin structure is
213 referred to as the A-type amylopectin or B-type amylopectin based on the criterion that
214 its starch granules show the A-type or B-type crystalline allomorph, such as wild-type or
215 *be2b* mutants, respectively (Nakamura et al., 2022). To characterize the structural features

216 of amylopectin, its chain-length distribution from a *japonica*-type line Kinmaze and an
217 *indica*-type line IR36 was measured and compared by the FACE method. Both chain
218 profiles have two major peaks; a large peak consisting of short chains of having DP 6 to
219 approximately 34 (A and B1 chains) and a small peak consisting of long chains having
220 $DP \geq$ approximately 37 (cluster-interconnecting B2-B4 chains) (Figs. 1A and 1B). Figs.
221 1C and 1D show that although both of their *be2b* mutant (*ae* mutant) lines EM10 and
222 IR36*ae* also had two major peaks, the proportion of long chains (B2-B4 chains) to short
223 chains (A and B1 chains) was markedly increased by the loss of BEIIb activity
224 (Supplementary Table S1).

225 Fig. 2 shows the differences in endosperm amylopectin chain-length distribution
226 between *japonica*-type and *indica*-type lines and between wild-type and *ae* type lines.
227 The amylopectin in *japonica*-type *ae* mutant line EM10 had fewer very short chains of
228 DP 6-12 with a peak of DP approximately 8-10 and more long chains of $DP \geq$ about 37
229 and intermediate chains of DP 14-30 compared with Kinmaze amylopectin (Fig. 2A).
230 Notably, the similar pattern of differences in chain-length distribution of amylopectin
231 between *indica*-type mutant line IR36*ae* and its wild-type line IR36 was detected,
232 although the extent of differences between *indica*-type lines was significantly lower than
233 that between *japonica*-type lines (Figs. 2A and 2B). The pattern of difference in chain-
234 length distribution of amylopectin between the SSIIa-deficient *japonica*-type rice and the
235 SSIIa-active *indica*-type rice was clearly different from that between the *ae*-mutant and
236 its wild-type (Compare Fig. 2B with Figs. 2A and 2C). The proportion of very short
237 chains of DP 6-10 was higher but that of intermediate chains of DP 13-24 was lower in a
238 *japonica*-type line Kinmaze than an *indica*-type line IR36, whereas there was no
239 significant difference of B2-B4 chains between two lines (Fig. 2B and Supplementary
240 Table S1), consistent with our previous studies (Umemoto et al., 1999; Nakamura et al.,
241 2002, 2005).

242

243 **3.2 Comparison of chain-length distribution of phosphorylase-limit dextrins (Φ -LD)** 244 **of amylopectin in mature endosperm of *be2b* mutant lines and their parent cultivars** 245 **of *japonica*-type rice and *indica*-type rice**

246

247 To examine the internal structure of amylopectin more in details, the external segments
248 of chains were digested by a rabbit muscle phosphorylase a (SIGMA) and then the chain-
249 length distribution of the resulting Φ -LD was determined by the FACE method. In this
250 analysis, almost all of the chains of DP 4 are considered to be derived from A chains.
251 According to this criterion, the amounts of A chains (DP 4-chains) were approximately

252 52%, 57%, 52%, and 55% in Kinmaze, EM10, IR36, and IR36ae, respectively (Fig. 3),
 253 indicating that the proportion of A chains in amylopectin was significantly higher in either
 254 *be2b* mutant than that in its wild-type. Fig. 4 compares the chain profiles of Φ -LD.
 255 Compared with wild-type Kinmaze, Φ -LD of its *be2b* mutant EM10 had fewer chains of
 256 DP 6-18 and enriched chains of DP 24-37 (Fig. 4A). The result suggests that the wild-
 257 type amylopectin had more branches inside the cluster, and therefore some chains carried
 258 multiple branched chains. This resulted in longer internal chain-length in Kinmaze
 259 amylopectin than EM10 amylopectin. Fig. 4B shows that Φ -LD from *japonica*-type
 260 Kinmaze had more A chains but slightly less short internal segments of DP 6-9 than that
 261 from *indica*-type IR36. This suggests that the IR36 amylopectin had slightly more B1
 262 chains with short internal segments of DP 6-9 to some extent than the Kinmaze
 263 amylopectin. Figure 5 illustrates the structural features of amylopectins of Kinmaze and
 264 IR36 and their *ae* mutants, although the difference of amylopectin between EM10 and
 265 IR36ae was too small to present it in the figure.

266

267 **3.3 X-ray diffraction (XRD) patterns of starch granules in in mature endosperm of** 268 ***be2b* mutant lines and their parent cultivars of *japonica*-type rice and *indica*-type** 269 **rice**

270

271 Fig. 6 shows the XRD profiles of various starch granules in mature endosperms of
 272 Kinmaze, IR36, EM10 and IR36ae. The XRD profile of Kinmaze (Fig. 6A) and IR36
 273 (Fig. 6B) had peaks at the scattering vector, q , of approximately 10.58 (a single peak),
 274 12.03 and 12.71 (doublet peaks), and 16.18 nm⁻¹ (a single peak), which are characteristics
 275 of A-type starch granules in cereal endosperm. On the other hand, the XRD profile of
 276 EM10 (Fig. 6C) and IR36ae (Fig. 6D) had peaks at q of approximately 3.724 (a single
 277 peak), 11.38 (a single peak), 15.54 and 16.92 nm⁻¹ (doublet peaks), which are
 278 characteristics of B-type starch granules (Nagasaki et al., 2021; Nakamura et al., 2022).

279

280 **3.4. Optical sum frequency generation (SFG) spectroscopy of starch granules in** 281 **mature endosperm of *be2b* mutant lines and their parent cultivars of *japonica*-type** 282 **rice and *indica*-type rice**

283

284 Figure 7 shows SFG spectra obtained for starch granules in mature endosperms of
 285 Kinmaze, EM10, IR36, and IR36ae. The curves represent the SFG intensity fit to
 286 Lorentzian curves in Eq. (1) below with fitting parameters in Table S1.

$$287 \quad |\chi^{SFG}|^2 = \left| \chi^{NR} + \sum_{n=1}^5 \frac{A_n \exp(i\theta_n)}{\omega - \omega_n + i\gamma_n} \right|^2 \quad (1)$$

288 Big peaks at around 2910 cm⁻¹ and 2970 cm⁻¹ were previously assigned to C-H and C-
289 H₂ stretching vibrations, respectively (Kouyama et al., 2016), but the appearance of the
290 separate peaks around 2870 cm⁻¹ suggests that we should reconsider the assignments. For
291 the present we assigned the peaks at 2870 cm⁻¹, 2910 cm⁻¹, and 2960 cm⁻¹ as CH or CH₂
292 vibrations. The broad peak around 3100cm⁻¹ was tentatively assigned to H₂O peak in our
293 previous paper (Nakamura et al., 2020).

294 In our previous paper (Nakamura et al., 2020) we reported that starch from the matured
295 endosperms of Kinmaze and EM10 show different SFG spectra according as they are A-
296 and B-type, respectively (Kong et al., 2014). This difference was reproduced in Fig. 7A
297 (Kinmaze) and 7B (EM10). Figures 7A and 7D, SFG spectra of starch granules in mature
298 endosperms of IR35, an *indica*-type cultivar, and IR36*ae*, a *be2b* mutant line of IR35, had
299 similar shapes to Figs. 7A and 7B, respectively. This tendency was also reflected in the
300 list of resonant frequencies in Supplementary Table S2. Namely, the SFG spectra of
301 Kinmaze and IR36 had three resonant oscillators between 2900 cm⁻¹ and 3000 cm⁻¹, while
302 those of EM10 and IR36*ae* have two. Thus, it was confirmed that the effect of BEIIb was
303 clearly correlated with the SFG spectral shapes.

304

305

306 4 DISCUSSION

307

308 4.1 The structural features of A-type and B-type amylopectin in rice endosperm

309

310 The present paper analyzed the fine structures of A-type and B-type amylopectins that
311 give rise to A-type and B-type crystals, respectively, of starch granules of rice (Figs. 1-
312 4). The results confirmed that both *japonica*-type and *indica*-type amylopectin had two
313 types of branches, while branches of their *be2b* mutant ones were present only in the
314 amorphous lamellae (Fig. 5), consistent with our previous study (Nakamura, 2002, 2015,
315 Nakamura et al., 2005, 2020, 2022). This model well explains the reason why the average
316 length of external segments of cluster chains is longer in the B-type amylopectin in *be2b*
317 mutants than that in the A-type amylopectin in their wild-types.

318 It is known that BEIIb is specifically expressed in rice endosperm, affecting the
319 structural features of amylopectin and crystalline properties of starch granules (Nishi et
320 al. 2001; Nakamura 2018; Nakamura et al. 2020; Ying et al. 2022). When BEIIb activity
321 was lost in the endosperm, chains of amylopectin became longer (Fig. 2), resulting in
322 formation of longer double helices, and this caused starch granules properties to be
323 resistant to thermal gelatinization and the crystalline allomorphs to change to the B-type

324 from the A-type, as determined by XRD (Fig. 6) and SFG analyses (Fig. 7), consistent
325 with our recent studies (Nakamura et al., 2020; Ying et al., 2022; Zhang et al., 2022) and
326 past investigations by other groups worldwide (Wei et al., 2010; Butardo et al., 2011).

327 328 **4.2 Structural boundary between the A-type amylopectin and the B-type** 329 **amylopectin**

330
331 Although amylopectin chains from an *indica*-type rice were longer than those from a
332 *japonica*-type amylopectin in wild-type, both starches showed A-type crystalline
333 allomorph (Figs. 6 and 7). The fine structure of amylopectin was very similar between
334 the *be2b* mutants generated from the *japonica*-type line EM10 and the *indica*-type line
335 IR36*ae* (Fig. 2D), and in fact their starch granules exhibited the B-type allomorph (Figs.
336 6 and 7). However, it is noted that in terms of chain-length profile, the *indica*-type IR36
337 amylopectin appeared to be more similar to the *be2b* mutant amylopectin compared with
338 the *japonica*-type Kinmaze one (Compare Fig. 2C with Fig. 2A, Supplementary Table
339 S1). The analysis of Φ -LD of amylopectin can give us an invaluable information on the
340 features of amylopectin internal structure as well as the proportion of and chain-length
341 distribution of A-chains. The Φ -LD of the *be2b* mutant amylopectin had depleted short
342 B chains of DP approximately 6-20 and more long B chains of DP about 24-37 compared
343 to wild-type amylopectin (Fig. 4A). The result suggests that B chains of the *be2b* mutant
344 amylopectin had longer internal segments than those of its wild-type amylopectin. This
345 is consistent with an assumption that B1 chains of wild-type amylopectin carry branches
346 inside (the crystalline lamellae) as well as amorphous lamellae of the cluster, whereas B
347 chains of the *be2b* mutant amylopectin have branches almost in the amorphous lamellae,
348 as illustrated in Fig. 5. This idea on the structural change of the cluster in the *ae* mutant
349 is consistent with the cluster structure proposed by Waigh et al., (2000) that the average
350 length of the amylopectin helices is longer in B-type starches compared with that in A-
351 type starches. The proportion of A chains was significantly higher in the *be2b* mutant
352 amylopectin than that in the wild-type amylopectin (Fig. 3 and 4). The results suggest
353 that new branches in the amorphous lamellae were more easily formed in B chains than
354 in A chains compared with those in the crystalline lamellae, because A chains become B
355 chains when they are used as acceptor chains.

356 Irrespective of phosphorolysis of amylopectin, number of total chains are unchanged. It
357 is also considered that the number of cluster-interconnecting chains is unchanged by the
358 treatment of amylopectin with phosphorylase. Therefore, amylopectin chain length
359 distribution can be extrapolated by adding chain-length of DP 12 to each chain of Φ -LD.

360 In this way, the hypothetical chain profiles for A chains can be calculated. Fig. 8 compares
361 the chain-length distribution of possible A chains of amylopectin from 4 lines used in this
362 study. If this hypothesis is correct, amylopectins of both wild-types and their *be2b* mutants
363 had A chains of DP approximately 6-18. Although it is known that short chains of $DP \leq 9$
364 are unable to form double helices (Gidley and Bulpin, 1987), the proportion of these short
365 chains in total amylopectin chains were only 15.7, 4.7, 7.8, and 4.7% in Kinmaze, EM10,
366 IR36, and IR36*ae*, respectively (Fig. 8). This shows that most of A chains of amylopectin
367 in these lines participated in the formation of double helices, facilitating crystalline
368 properties of starch granules. However, it is noted that the proportion of these chains of
369 DP 6-9 was greatly lower while the proportion of DP 10-18 chains and in particular, that
370 of DP 17 and 18 chains were significantly higher in the *be2b* (*ae*) mutants than that in
371 wild-types. The results indicate that *be2b* mutant amylopectin had longer double helices
372 than wild-type amylopectin. Therefore, it is concluded that all these structural features of
373 amylopectin determined starch granules to be the A-type or the B-type crystalline
374 allomorph. It is widely known that that the crystal type of starch is largely dependent of
375 length of external segments of amylopectin. Generally, shorter chains favor the formation
376 of A-type allomorph whereas longer chains contribute to the formation of B-type
377 allomorph (Hizukuri et al., 1983; Hizukuri, 1996). It was also shown that amylose chains
378 of DP 10-13 exhibit A-type crystals, while those of $DP \geq 14$ yield B- or C-type crystals
379 (Gidley and Bulpin, 1987; Pfannemüller, 1987). The ratio of number of chains DP10-
380 13/number of chains of 13-18 was calculated to be approximately 1.59 and 1.30 in
381 possible A-chains from Kinmaze and IR36, respectively, whereas that was approximately
382 0.97 and 0.87 in those from EM10 and IR36*ae*, respectively (Fig. 8), consistent with
383 results reported previously cited above. In summary, it was confirmed that the length of
384 external segments of chains of amylopectin is a determinant of the crystalline allomorph
385 of starch granules.

386 Based on the present results, firstly, the average length of external segments of cluster
387 chains with DP up to approximately 24 greatly affects the type of crystalline allomorph
388 of starch granules. Secondly, it can be also pointed out that the presence of second
389 branches in the cluster synthesized by BEIIb would play an important role in the
390 crystallization of amylopectin double helices in the A-type crystal. Currently, it is well
391 known that *ae* starch is highly resistant to thermal gelatinization and hydrolysis by
392 hydrolytic enzymes compared to other starches (Tsuiki et al., 2018; Wang et al., 2017;
393 Nakamura, 2018), and therefore a better understanding of the relationship between
394 structures and functional properties of starches having various structures will be
395 important for the use of starch for food and industrial applications.

396

397

398 **5 CONCLUSION**

399

400 The present study aimed to examine the structural features of A-type or B-type
401 amylopectin which are responsible for the A-type or B-type crystals, respectively, of
402 starch granules by using starches in *japonica* and *indica* rice wild-type varieties and their
403 *be2b* (*ae*) mutants, because it is known that any wild-type varieties of cereals so far
404 examined have A-type starch crystals in their endosperm whereas their *be2b* (*ae*) mutants
405 produce B-type starch crystals (Hizukuri, 1996; Shannon et al., 2009). The present
406 comparative studies with starches from both *japonica*-type and *indica*-type rice wild-type
407 varieties and their *be2b* mutants could provide us with useful criteria to distinguish A-
408 type amylopectin from B-type amylopectin, because it is widely known that the fine
409 structure of amylopectin in starch from *japonica*- and *indica*-type rice endosperm greatly
410 differs from each other (Umemoto et al., 1999; Nakamura et al., 2002, 2005). Analysis of
411 the chain-length distribution of component chains of amylopectin and their Φ -LD
412 (internal chains) indicated that the average length of cluster chains (A and B1 chains) of
413 amylopectin was clearly longer in B-type amylopectin found in both *be2b* mutants than
414 that in A-type amylopectin formed in their wild-types (Figs. 1-4 and Supplementary Table
415 S1). The results can be explained by a specific role of BEIIb in the formation of the second
416 branches inside the cluster. In the *be2b* mutants the second branches were deficient in the
417 amylopectin cluster, and thus the average length of cluster chains became longer than that
418 in wild-types (Fig. 5). On the other hand, although chain-length of cluster chains in IR36
419 amylopectin was apparently longer than that in Kinmaze amylopectin (Fig. 2B), both
420 amylopectins were considered to have the second branches formed by BEIIb as well as
421 the first branches formed mainly by BEI, as presented by Figs. 5A and 5B. The present
422 study strongly suggests that the second branches synthesized by BEIIb would play an
423 important role in allying double helices of amylopectin in compact and regular manner,
424 and this results in the crystallization of amylopectin chains in the A-type allomorph. This
425 study claims that not only the average chain-length of cluster chains but also the presence
426 of the second branches in the cluster are important for the A-type crystalline allomorph
427 of starch granules.

428

429

430 **ACKNOWLEDGEMENTS**

431 We thank Dr. Hikaru Satoh for providing us with EM10 as the experimental material. We
432 also Dr. Naoko Fujita for help to use facilities in Akita Prefectural University. This study
433 was funded by JSPS KAKENHI Grant Number JP19H05721 (GMa).

434

435

436 **REFERENCES**

437

438 Buléon, A., Colonna, P., Plachot, V., & Ball, S. (1998). Starch granules: Structure and
439 biosynthesis. *International Journal of Biological Macromolecules*, *23*, 85-112.

440 Butardo, V.M., Fitzgerald, M.A., Bird, A.R., Gidley, M.J., Flanagan, B.M., Larroque, O.,
441 Resurreccion, A.P., Laidlaw, H.K.C., Jobling, S.A., Morell, M.K. & Rahman, S. (2011).
442 Impact of down-regulation of starch branching enzyme IIb in rice by artificial
443 microRNA- and hairpin RNA-mediated RNA silencing. *Journal of Experimental*
444 *Botany*, *62*, 4927-4941.

445 French, D. (1972). Fine structure of starch and its relationship to the organization of starch
446 granules. *Journal of Japanese Society of Starch Science*, *19*, 8-25.

447 French, D. (1984). Organization of starch granules, In R.L. Whistler, J.N. BeMiller, and
448 E. Paschall (Eds.), *Starch: Chemistry and Technology, second ed.* (pp. 183-247). San
449 Diego, New York, Boston, London, Sydney, Tokyo, and Toronto: Academic Press.

450 Gérard, C., Planchot, V., Colonna, P. & Bertoft, E. (2000). Relationship between
451 branching density and crystalline structure of A- and B-type maize mutant starches.
452 *Carbohydrate Research*, *326*, 130-144.

453 Gidley, M.J. & Bulpin, P.V. (1987). Crystallization of malto-oligosaccharides at models
454 of the crystalline forms of starch. *Carbohydrate Research*, *161*, 291-300.

455 Hieu, H.C., Li, H., Miyauchi, Y., Mizutani, G., Fujita, N. & Nakamura, Y. (2015). Wetting
456 effect on optical sum frequency generation (SFG) spectra of D-glucose, D-fructose,
457 and sucrose. *Spectrochimica Acta A138*, 834-839.

458 Hizukuri, S. (1986). Polymodal distribution of the chain lengths of amylopectin, and its
459 significance. *Carbohydrate Research*, *147*, 342-347.

460 Hizukuri, S. (1996). Starch: Analytical aspects. In A.-C. Eliasson (Ed.), *Carbohydrates*
461 *in Food* (pp. 347-429). Marcel Dekker, Inc.: New York, Basel, and Hong Kong.

462 Hizukuri, S., Kaneko, T. & Takeda, Y. (1983). *Biochimica Biophysica Acta*, *760*, 188-191.

463 Imberty, A., Buléon, A., Tran, V. & Pérez, S. (1991). Recent advances in knowledge of
464 starch structure. *Starch/Stärke*, *43*, 375-384.

465 Jane, J.L., Wong, K.S. & McPherson, A.E. (1997). Branch-structure difference in starches
466 of A- and B-type X-ray patterns revealed by their Naegeli dextrans. *Carbohydrate*
467 *Research*, 300, 219-227.

468 Kainuma, K. & French, D. (1972). Naegeli amylopectin and its relationship to starch
469 granule structure. II. Role of water in crystallization of B-starch. *Biopolymers*, 11,
470 2241-2250.

471 Kong, L., Lee, C., Kim, S.H. & Ziegler, G.R. (2014). Characterization of starch
472 polymorphic structures using vibrational sum frequency generation spectroscopy.
473 *Journal of Physical Chemistry. B* 118, 1775-1783.

474 Kouyama, W., Nishida, T., Hien, K.T.T., Mizutani, G., Hasegawa, H. & Miyamura, H.
475 (2016). Optical sum frequency generation spectroscopy of cracked non-glutinous rice
476 (*Oryza sativa* L.) kernels. *Journal of Biomaterial Nanobiotechnology*, 7, 13-18.

477 Miyauchi, Y., Sano, H. & Mizutani, G. (2006). Selective observation of starch in a water
478 plant using optical sum-frequency microscopy. *Journal of Optical Society of America.*
479 *A* 23, 1687-1690.

480 Nagasaki, A., Matsuba, G., Ikemoto, Y., Moriwaki, T., Ohta, N. & Osaki, K. (2021).
481 Analysis of the sol and gel structures of potato starch over a wide spatial scale. *Food*
482 *Science and Nutrition*, 9, 4916-4926.

483 Nakamura, Y. (2002). Towards a better understanding of the metabolic system for
484 amylopectin biosynthesis in plants: Rice endosperm as a model tissue. *Plant & Cell*
485 *Physiology*, 43, 718-725.

486 Nakamura, Y. (2015). Biosynthesis of reserve starch. In Y. Nakamura (Ed.), *Starch:*
487 *Metabolism and Structure* (pp. 161-209). Springer: Tokyo, Heidelberg, New York,
488 Dordrecht, London.

489 Nakamura, Y. (2018). Rice starch biotechnology: Rice endosperm as a model of cereal
490 endosperms. *Starch/Stärke*, 70, 1600375.

491 Nakamura, Y., Sakurai, A., Inaba, Y., Kimura, K., Iwasawa, N. & Nagamine, T. (2002).
492 The fine structure of amylopectin in endosperm from Asian cultivated rice can be
493 largely classified into two classes. *Starch/Stärke*, 54, 117-131.

494 Nakamura, Y., Francisco, Jr. P.B., Hosaka, Y., Sato, A., Sawada, T., Kubo, A. & Fujita, N.
495 (2005). Essential amino acids of starch synthase IIa differentiate amylopectin structure
496 and starch quality between *japonica* and *indica* rice varieties. *Plant Molecular Biology*,
497 58, 213-227.

498 Nakamura, Y., Ono, M., Hatta, T., Kainuma, K., Yashiro, K., Matsuba, G., Matsubara, A.,
499 Miyazato, A. & Mizutani, G. (2020). Effects of BEIIb-deficiency on the cluster

500 structure of amylopectin and the internal structure of starch granules in endosperm and
501 culm of *japonica*-type rice. *Frontiers in Plant Science*, *11*, 571346.

502 Nakamura, Y. & Kainuma, K. (2022). On the cluster structure of amylopectin. *Plant*
503 *Molecular Biology*, *108*, 291-306.

504 Nakamura, Y., Kubo, A., Ono, M., Yashiro, K., Matsuba, G., Wang, Y., Matsubara, A.,
505 Mizutani, G., Matsuki, J. & Kainuma, K. (2022). Changes in fine structure of
506 amylopectin and internal structures of starch granules in developing endosperms and
507 culms caused by starch branching enzyme mutations of *japonica* rice. *Plant Molecular*
508 *Biology*, *108*, 481-496.

509 Nishi, A., Nakamura, Y., Tanaka, N. & Satoh, H. (2001). Biochemical and genetic analysis
510 of the effects of *amylose-extender* mutation in rice endosperm. *Plant Physiology*, *127*,
511 459-472.

512 Ohdan, T., Francisco, Jr. P.B., Sawada, T., Hirose, T., Terao, T., Satoh, H. & Nakamura,
513 Y. (2005). Expression profiling of genes involved in starch synthesis in sink and source
514 organs of rice. *Journal of Experimental Botany*, *56*, 3229-3244.

515 O'Shea, M.G., Samuel, M.S., Konik, C.M. & Morell, M.K. (1998). Fluorophore-assisted
516 carbohydrate electrophoresis (FACE) of oligosaccharides: Efficiency of labeling and
517 high-resolution separation. *Carbohydrate Research*, *307*, 1-12.

518 Peat, S., Whelan, W.J. & Thomas, G.J. (1952). Evidence of multiple branching in waxy
519 maize starch. *Journal of Chemical Society*, 4546-4548.

520 Pfannemüller, B. (1987). *International Journal of Biological Macromolecules*, *9*, 105-
521 108.

522 Sawada, T., Nakamura, Y., Ohdan, T., Saitoh, A., Francisco, Jr., P.B., Suzuki, E., Fujita,
523 N., Shimonaga, T., Fujiwara, S., Tsuzuki, M., Colleoni, C. & Ball, S. (2014). Diversity
524 of reaction characteristics of glucan branching enzymes and the fine structure of α -
525 glucan from various sources. *Archives of Biochemistry and Biophysics*, *562*, 9-21.

526 Shannon, J.C., Garwood, D.L. & Boyer, C.D. (2009). Genetics and physiology of starch
527 development. In J. BeMiller and R. Whistler (Eds.), *Starch, Chemistry and Technology*,
528 *3rd ed.* (pp. 23-82). Academic Press: New York.

529 Tanaka, N., Fujita, N., Nishi, A., Satoh, H., Hosaka, Y., Ugaki, M., Kawasaki, S. &
530 Nakamura, Y. (2004). The structure of starch can be manipulated by changing the
531 expression levels of starch branching enzyme IIb in rice endosperm. *Plant*
532 *Biotechnology Journal*, *2*, 507-516.

533 Tsuiki, K., Fujisawa, H., Itoh, A., Sato, M. & Fujita, N. (2016). Alterations of starch
534 structure lead to increased resistant starch of steamed rice: Identification of high
535 resistant starch line lines. *Journal of Cereal Science*, *68*, 88-92.

- 536 Umemoto, T., Nakamura, Y., Satoh, H. & Terashima, K. (1999). Differences in
537 amylopectin structure between two rice varieties in relation to the effects of
538 temperature during grain-filling. *Starch/Stärke*, 51, 58-62.
- 539 Umemoto, T., Yano, M., Satoh, H., Shomura, A. & Nakamura, Y. (2002). Mapping of a
540 gene responsible for the difference in amylopectin structure between *japonica*-type and
541 *indica*-type rice varieties. *Theoretical Applied Genetics*, 104, 1-8.
- 542 Waigh, T.A., Gidley, M.J., Komanshek, B. & Donald, A.M. (2000). The phase
543 transformations in starch during gelatinization: a liquid crystalline approach.
544 *Carbohydrate Research*, 328, 165-176.
- 545 Wang, J., Hu, P., Chen, Z., Liu, Q. & Wei, C. (2017). Progress in high-amylose cereal
546 crops through inactivation of starch branching enzyme. *Frontiers in Plant Science*, 8,
547 469.
- 548 Wei, C., Xu, B., Qin, F., Yu, H., Chen, C., Meng, X., Zhu, L., Wang, Y., Gu, M. & Liu,
549 Q. (2010). C-type starch from high-amylose rice resistant starch granules modified by
550 antisense RNA inhibition of starch branching enzyme. *Agricultural Food Chemistry*,
551 58, 7383-7388.
- 552 Yamaguchi, M., Kainuma, K. & French, D. (1979). Electron microscopic observations of
553 waxy maize starch. *Journal of Ultrastructural Research*, 69, 249-261.
- 554 Yano, M., Okuno, K., Kawakami, J., Satoh, H. & Omura, T. (1985). High amylose
555 mutants of rice, *Oryza sativa* L. *Theoretical Applied Genetics*, 69, 253-257.
- 556 Ying, Y., Zhang, Z., Tappiban, P., Xu, F., Deng, G., Dai, G. & Bao, J.S. (2022). Starch
557 fine structure and functional properties during seed development in BEIIb active and
558 deficient rice. *Carbohydrate Polymers*, 292, 119640.
- 559 Zhang, Z., Hu, Y., Zhao, J., Zhang, Y., Ying, Y., Xu, F. & Bao, J.S. (2022). The role of
560 different *Wx* and *BEIIb* allele combinations on fine structures and functional properties
561 of *indica* rice starches. *Carbohydrate Polymers*, 278, 118972.

562
563
564

565 SUPPORTING INFORMATION

566 Additional supporting information can be found online in the Supporting Information
567 section at the end of this article.

568
569
570
571
572

573 **Legends for figures**

574

575 **Fig. 1** Chain-length distribution of amylopectin in mature endosperms of a wild-type
576 *japonica* cultivar Kinmaze, a wild-type *indica* cultivar IR36, and their *be2b* mutant lines,
577 EM10 and IR36ae, respectively. The vertical axis presents the proportion (molar %) of
578 the amount of each chain to the total amounts of chains with degree of polymerization
579 (DP) from 6 to 90, whereas the horizontal axis shows the DP value of the chain.
580 Amylopectin of Kinmaze (A), IR36 (B), EM10 (C), and IR36ae (D). The experiments
581 were repeated at least three times until all these results were consistent, whereas each
582 figure shows one representative result. Values are the averages calculated from three
583 replicate measurements. Standard deviations were too small to be shown in the figure.

584

585

586 **Fig. 2** Difference in amylopectin between EM10 and Kinmaze, calculated from data of
587 EM10 subtracted by those of Kinmaze. A, Difference in amylopectin between EM10 and
588 Kinmaze, calculated from data of EM10 subtracted by those of Kinmaze. B, Difference
589 in amylopectin between Kinmaze and IR36, calculated from data of Kinmaze subtracted
590 by those of IR36. C, Difference in amylopectin between IR36ae and IR36, calculated
591 from data of IR36ae subtracted by those of IR36. D, Difference in amylopectin between
592 EM10 and IR36ae, calculated from data of EM10 subtracted by those of IR36ae. The
593 other conditions are the same as in Fig. 1.

594

595

596 **Fig. 3** Chain-length distribution of phosphorylase-limit dextrans (Φ -LD) of amylopectin
597 in mature endosperms of a wild-type *japonica* cultivar Kinmaze, a wild-type *indica*
598 cultivar IR36, and their *be2b* mutant lines, EM10 and IR36ae, respectively. Φ -LD of
599 Kinmaze (A), IR36 (B), EM10 (C), and IR36ae (D). The other conditions are the same as
600 in Fig. 1, except that data were obtained for chains with degree of polymerization (DP)
601 from 4 to 60.

602

603

604 **Fig. 4** Comparison of chain-length distribution of Φ -LD of amylopectin in mature
605 endosperms of a wild-type *japonica* cultivar Kinmaze, its *be2b* mutant line, EM10, a
606 wild-type *indica* cultivar IR36, and its *be2b* mutant line, IR36ae. A, Difference in Φ -LD
607 between EM10 and Kinmaze, calculated from data of EM10 subtracted by those of
608 Kinmaze. B, Difference in Φ -LD between Kinmaze and IR36, calculated from data of

609 Kinmaze subtracted by those of IR36. C, Difference in Φ -LD between EM10 and IR36ae,
610 calculated from data of EM10 subtracted by those of IR36ae. The other conditions are the
611 same as in Fig. 3.

612

613

614 **Fig. 5** A schematic representation of the hypothetical cluster structure of amylopectin in
615 endosperm from a wild-type *japonica* cultivar Kinmaze (A), a wild-type *indica* cultivar
616 IR36 (B), and their *be2b* mutant lines, EM10 (C) and IR36ae (D), respectively.

617

618

619 **Fig. 6** Wide angle X-ray scattering (WAXS) analysis of starch granules in mature
620 endosperms from a wild-type *japonica* cultivar Kinmaze (A), a wild-type *indica* cultivar
621 IR36 (B), and their *be2b* mutant lines, EM10 (C) and IR36ae (D), respectively. See
622 **Materials and methods** in details.

623

624

625 **Fig. 7** SFG spectra of starch granules in mature endosperms from a wild-type *japonica*
626 cultivar Kinmaze (A), a wild-type *indica* cultivar IR36 (B), and their *be2b* mutant lines,
627 EM10 (C) and IR36ae (D), respectively. See **Materials and methods** in details.

628

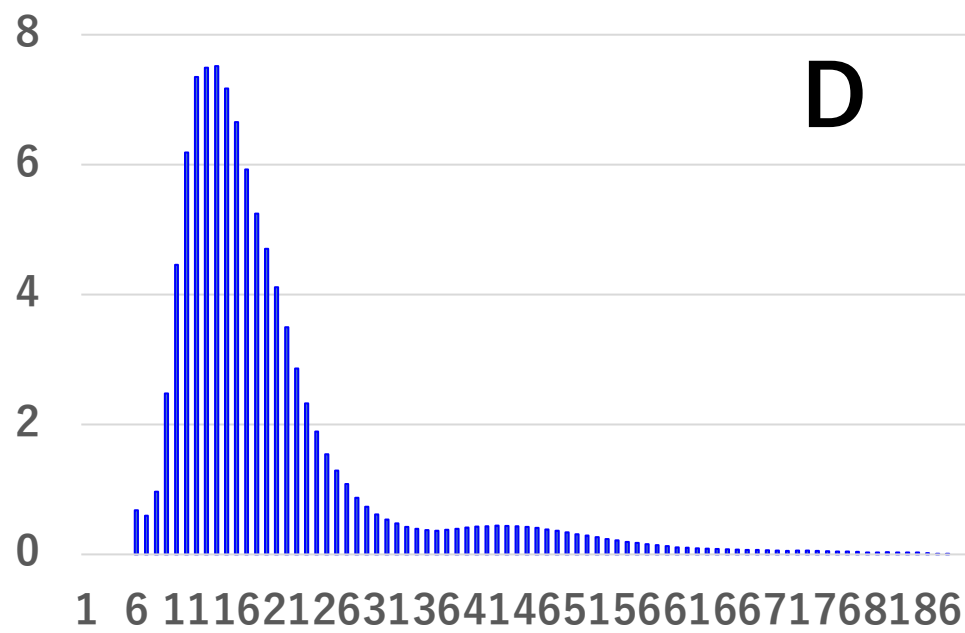
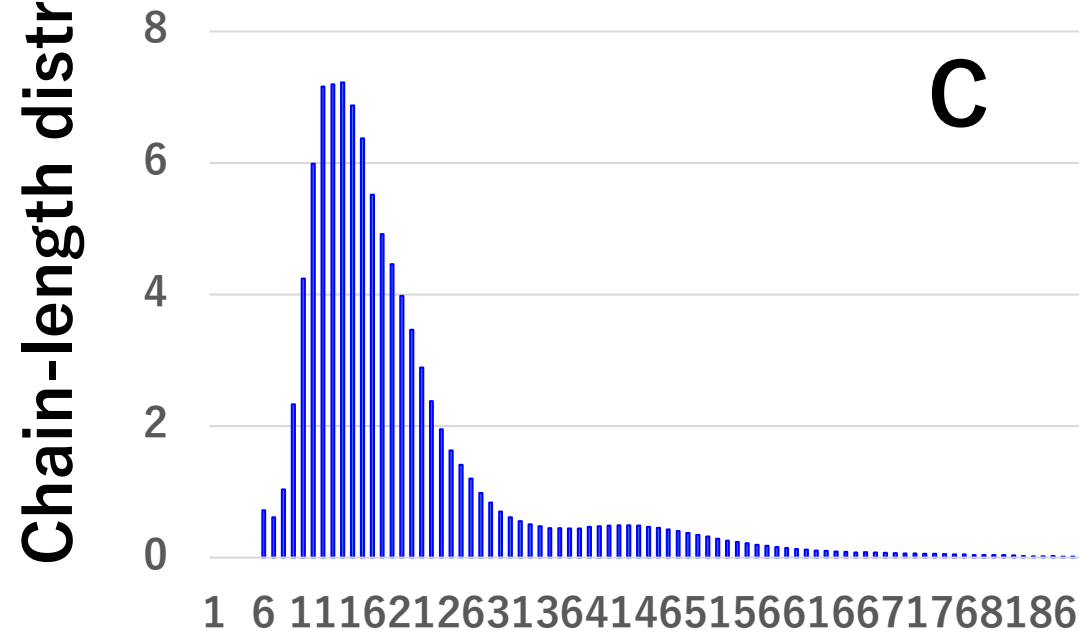
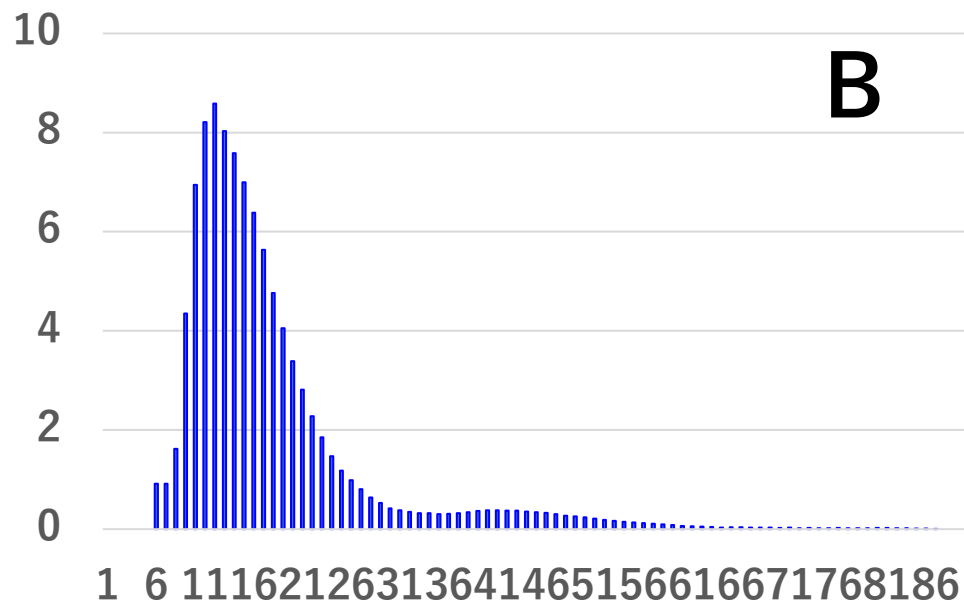
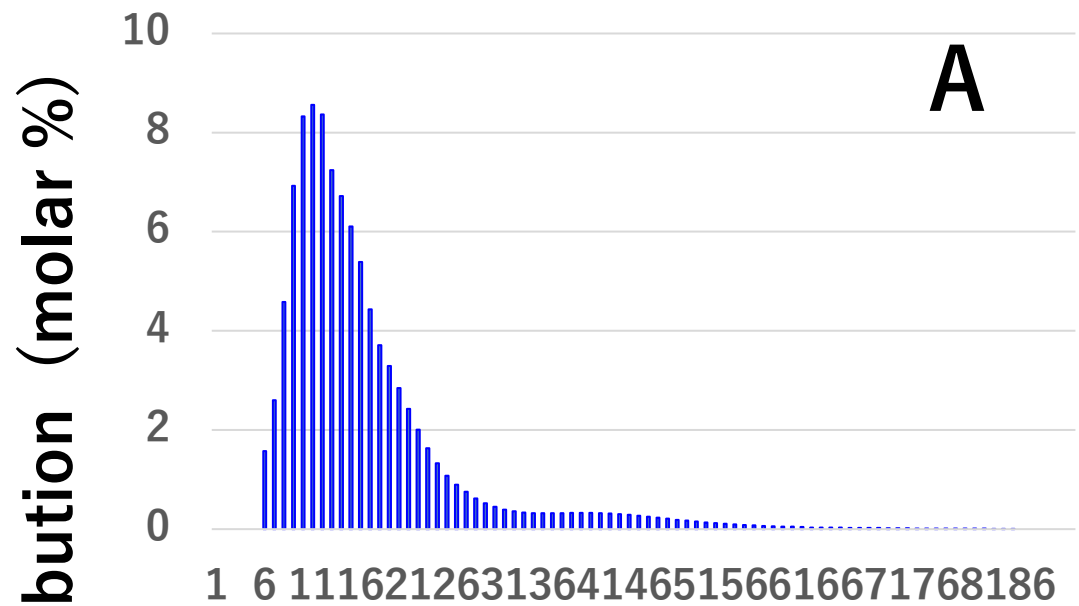
629

630 **Fig. 8** The hypothetical chain-length distribution of A chains in a wild-type *japonica*
631 cultivar Kinmaze (A), a wild-type *indica* cultivar IR36 (B), and their *be2b* mutant lines,
632 EM10 (C) and IR36ae (D), respectively. The chain-length distribution of hypothetical A
633 chains in the DP range of 6-18 were obtained by the difference of chain-length distribution
634 between native amylopectin (DP 6-60) and its Φ -LD (DP ≥ 5), although each DP of Φ -
635 LD was added by DP12. See text in details.

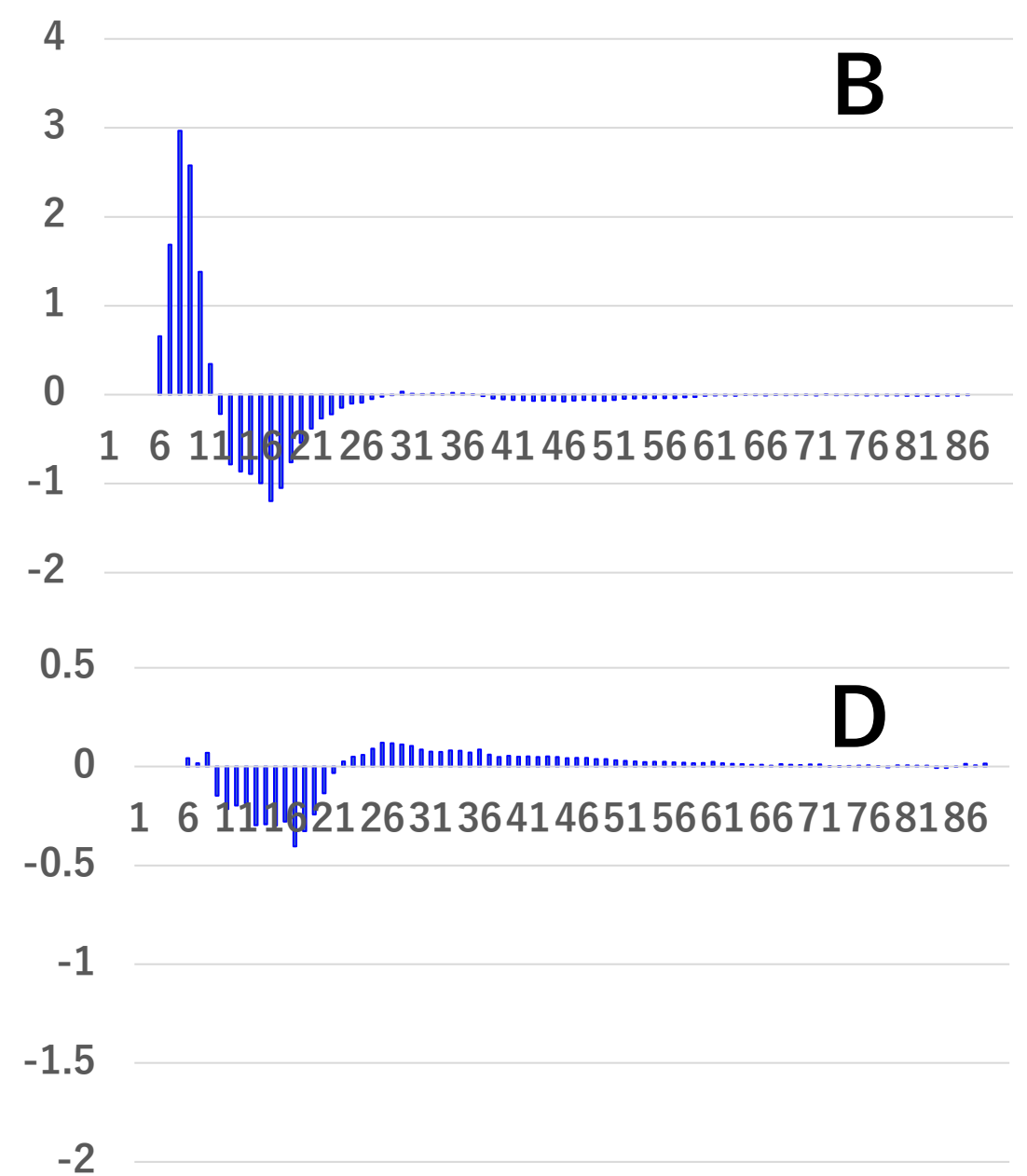
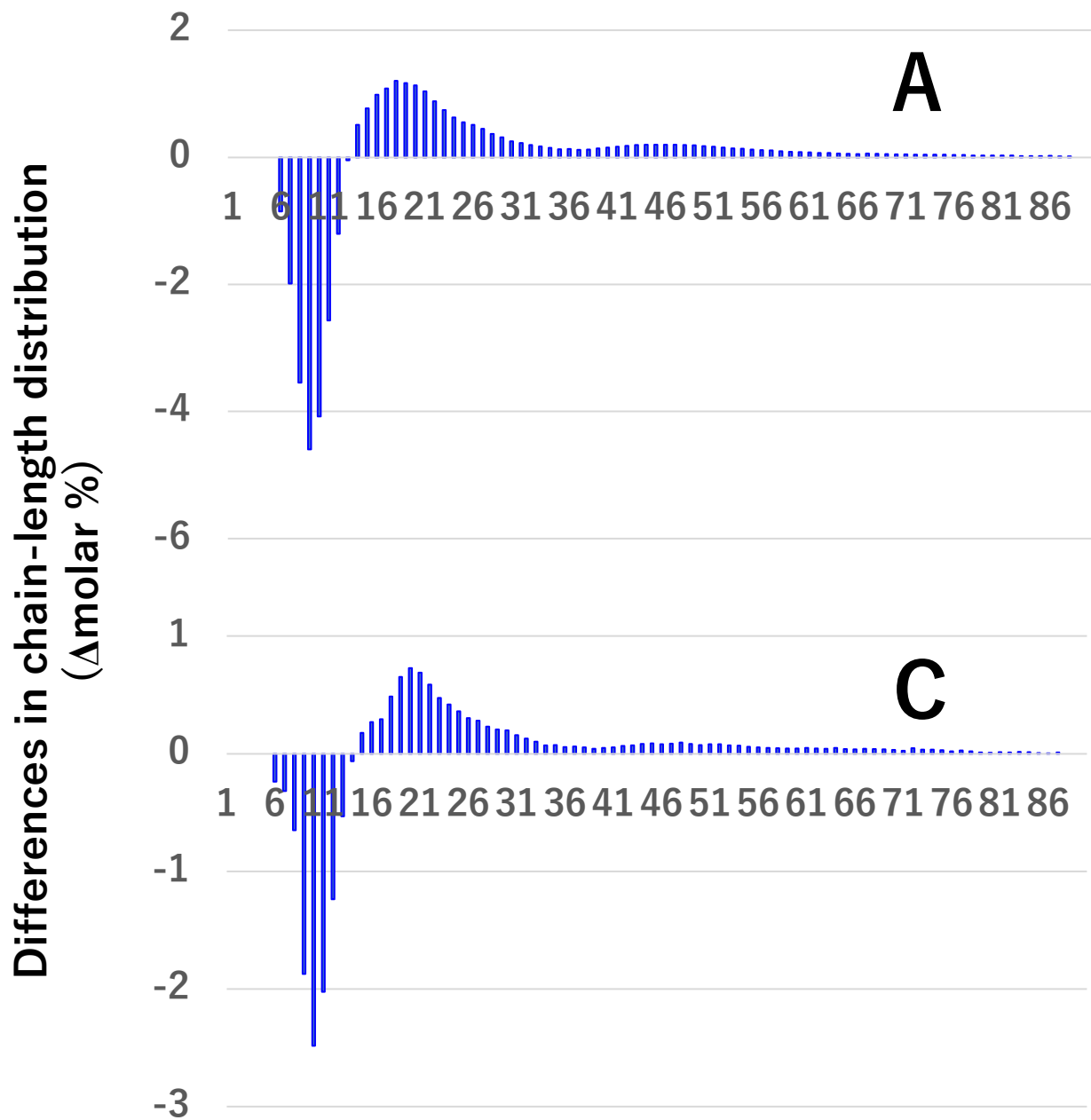
636

637

638

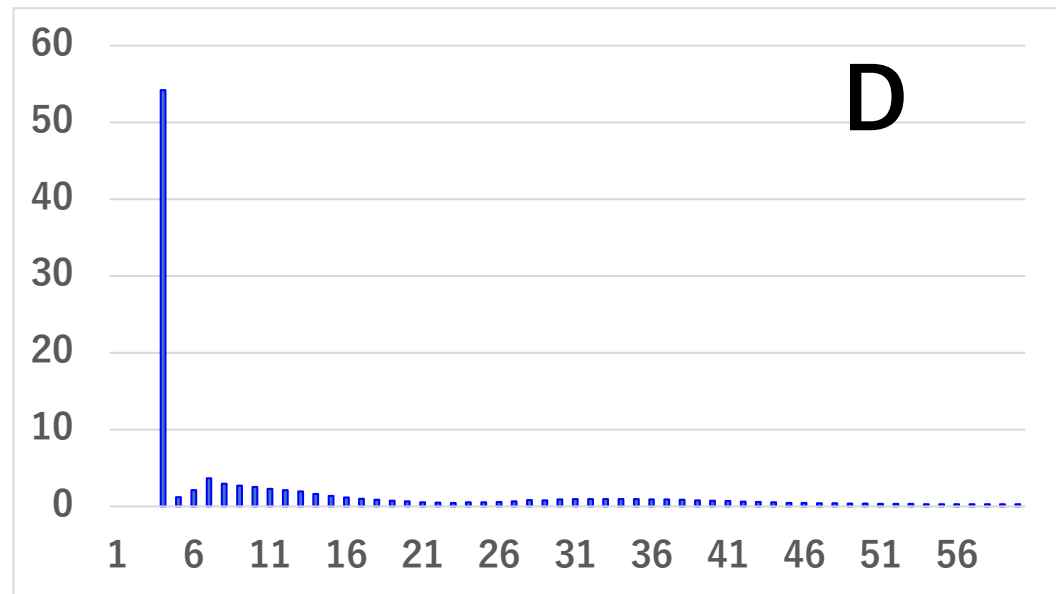
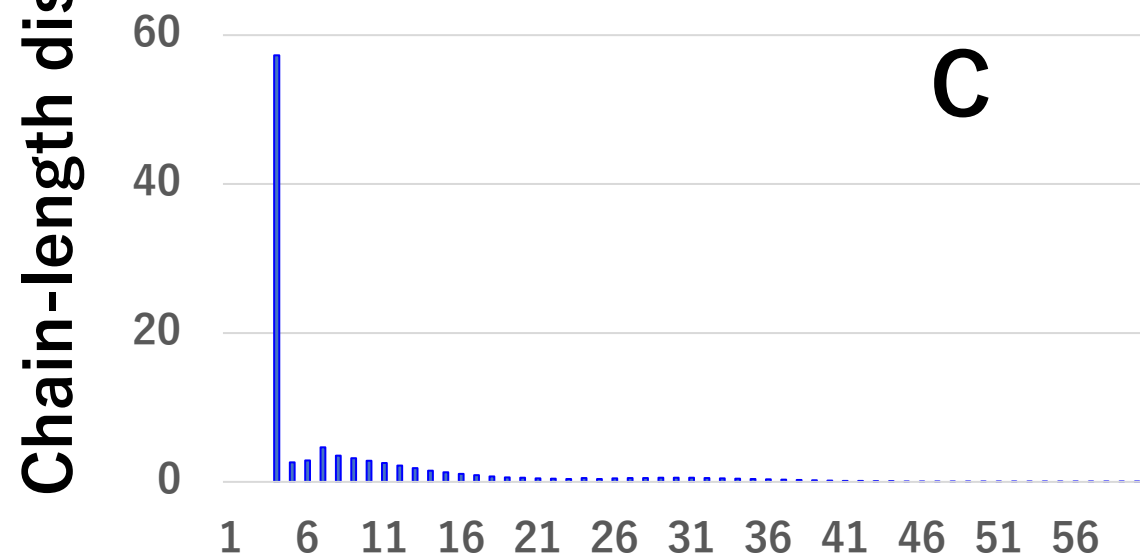
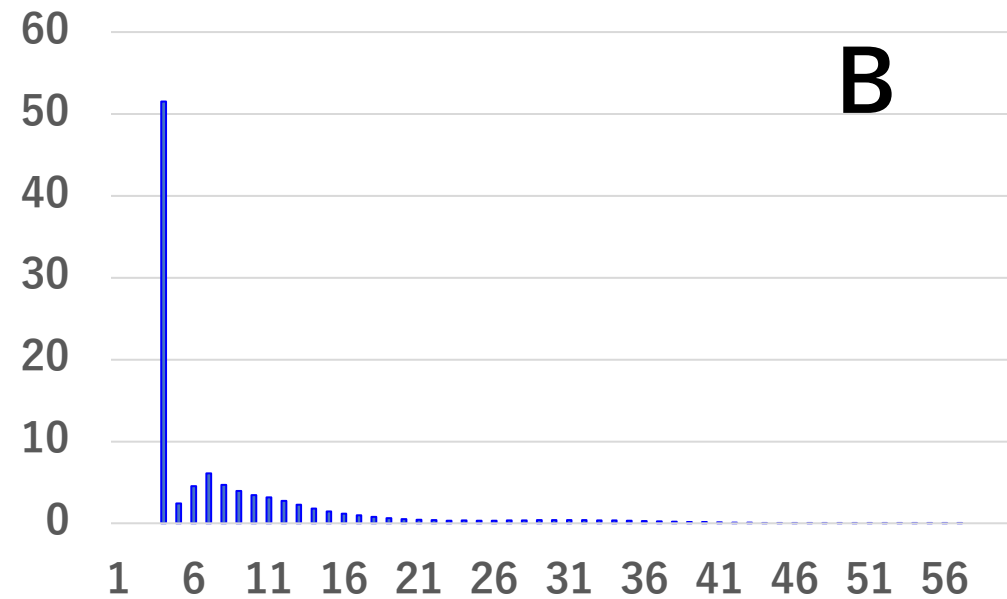
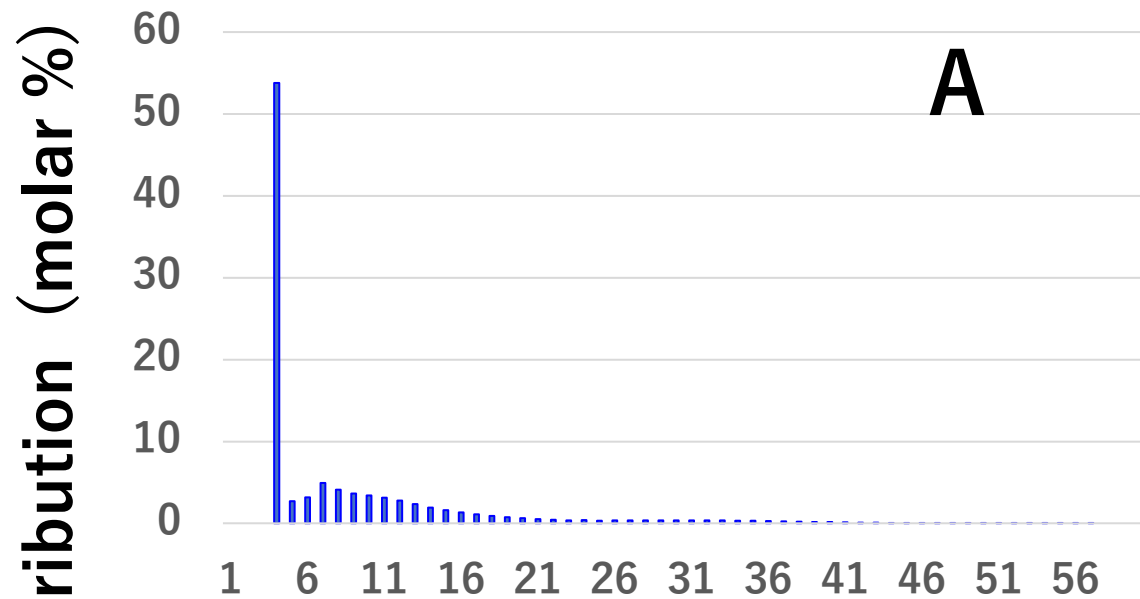


Degree of polymerization (DP)



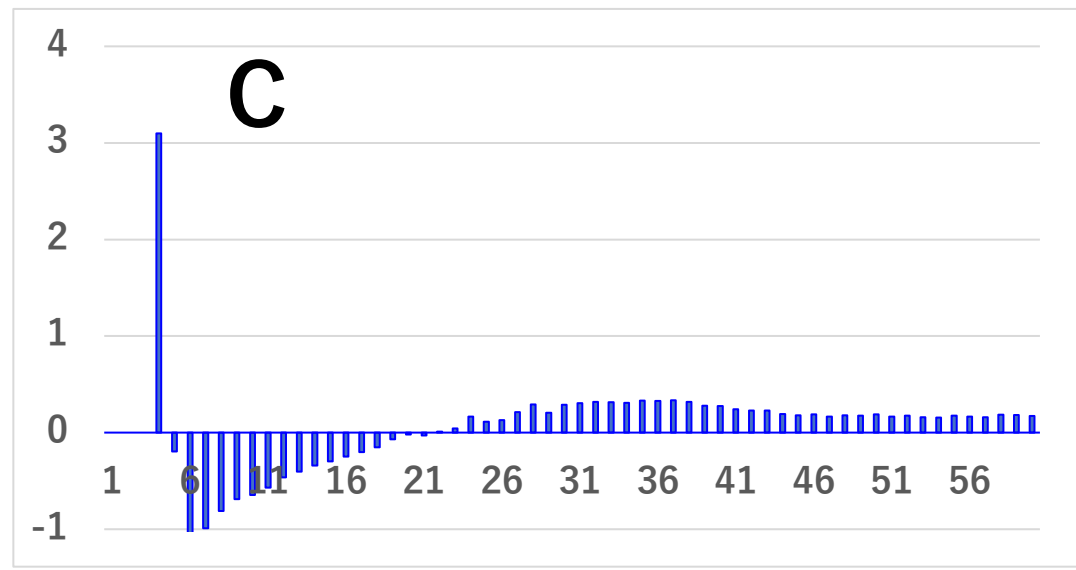
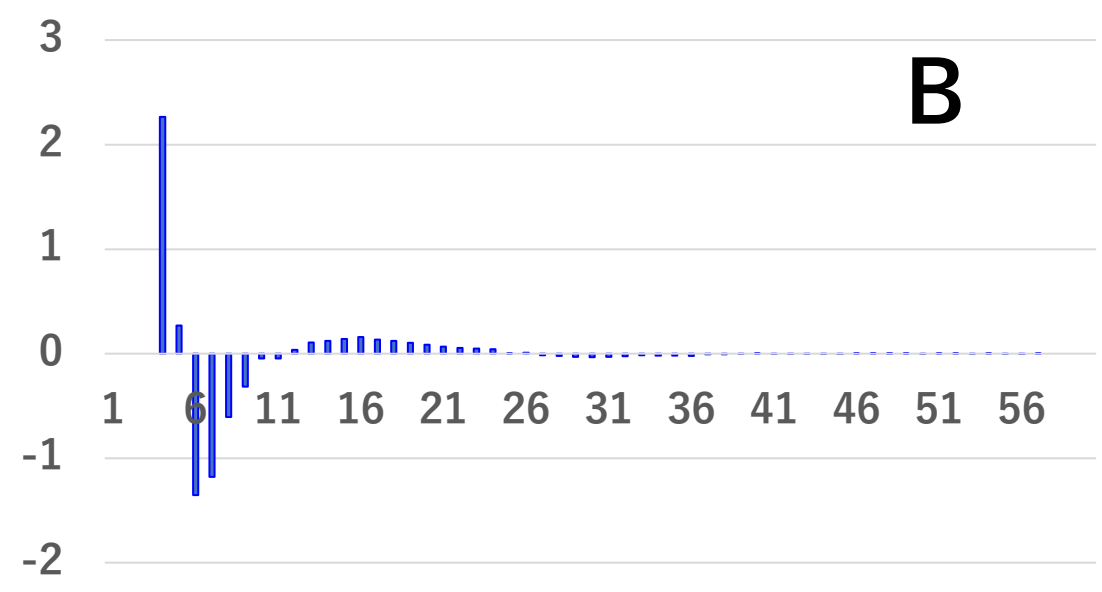
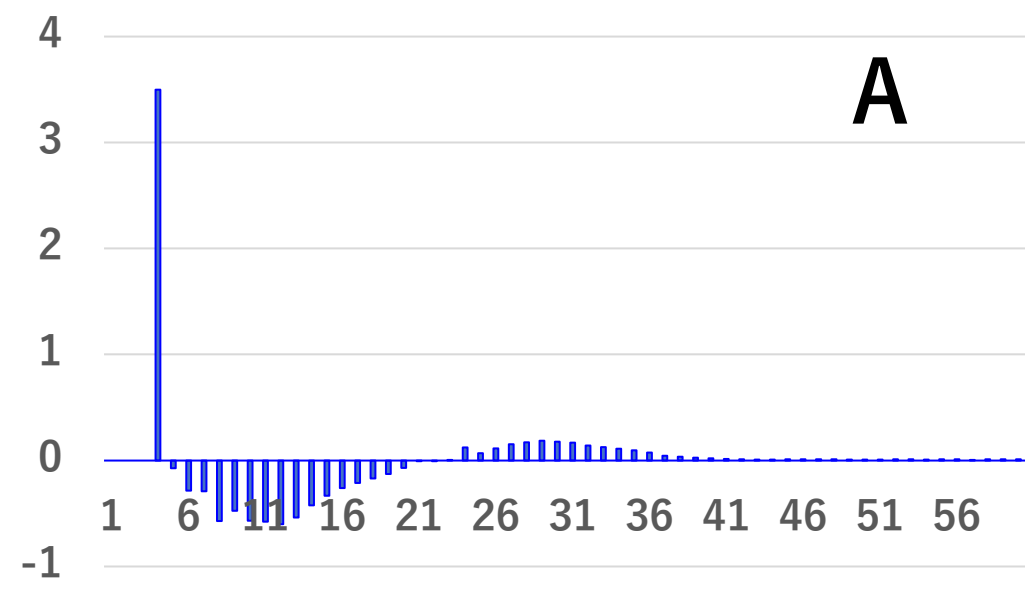
Degree of polymerization (DP)

Fig. 3

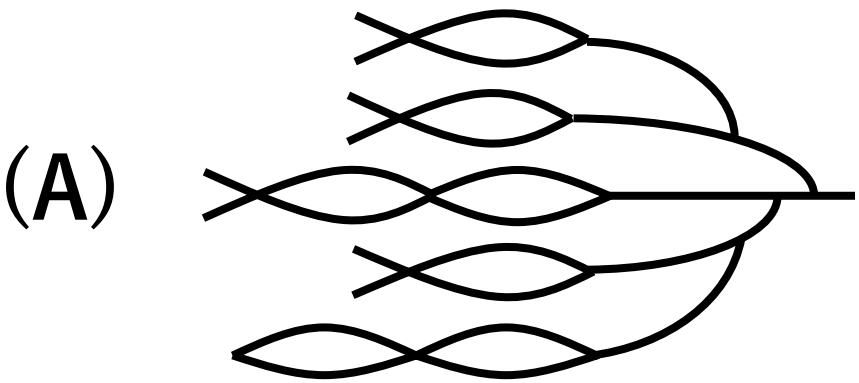


Degree of polymerization (DP)

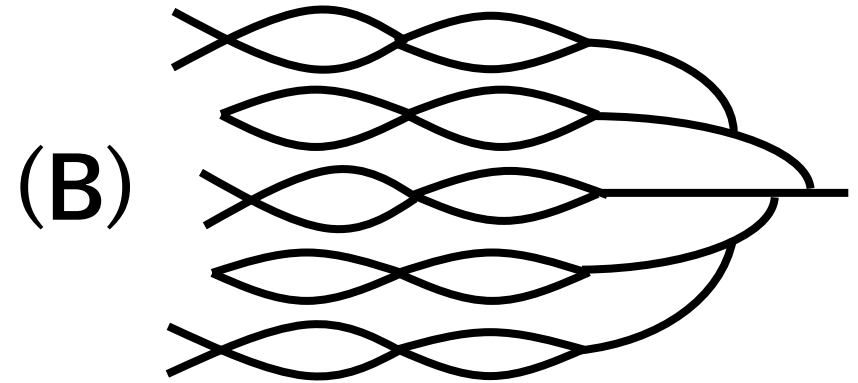
Differences in chain-length distribution
(Δ molar %)



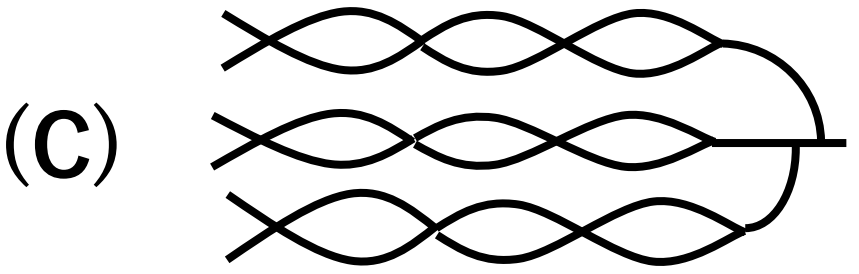
Degree of polymerization (DP)



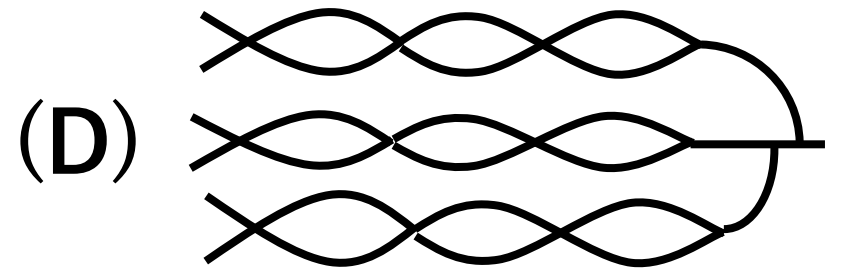
Kinmaze (*japonica*)



IR36 (*indica*)

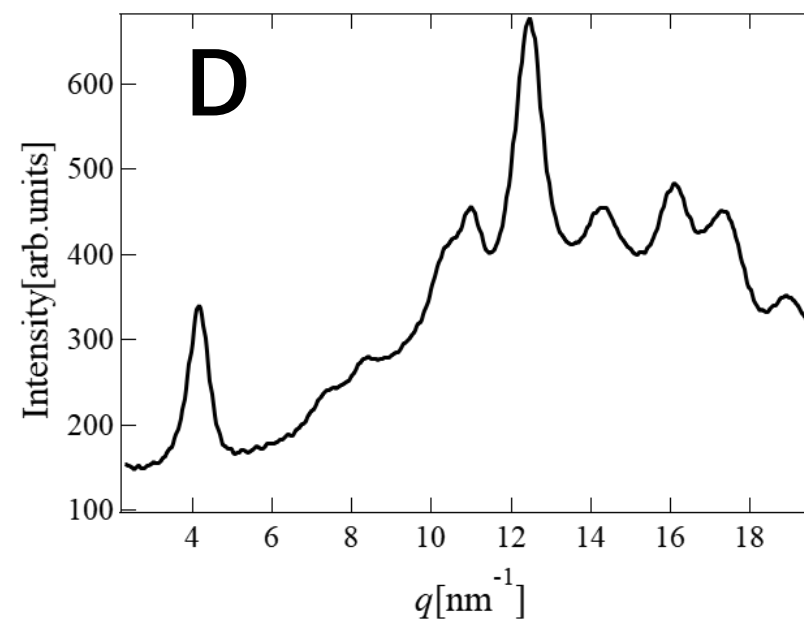
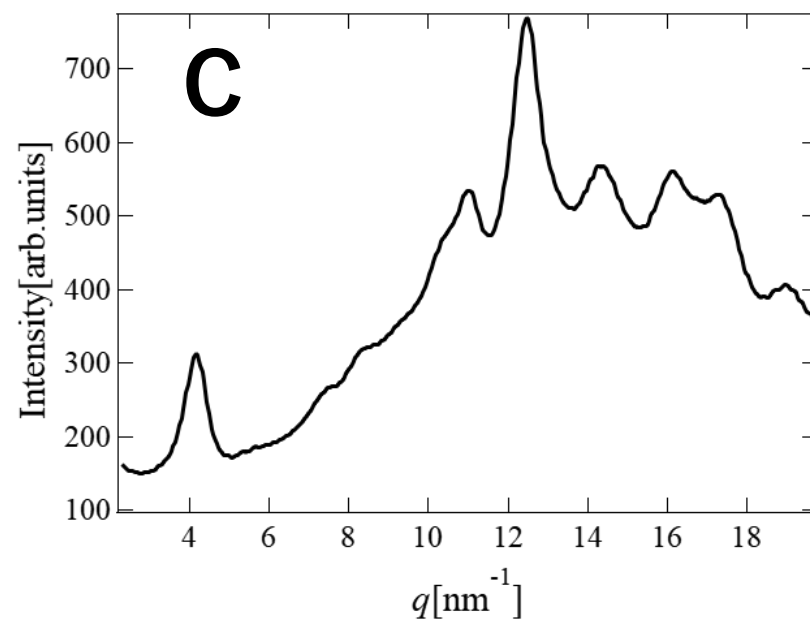
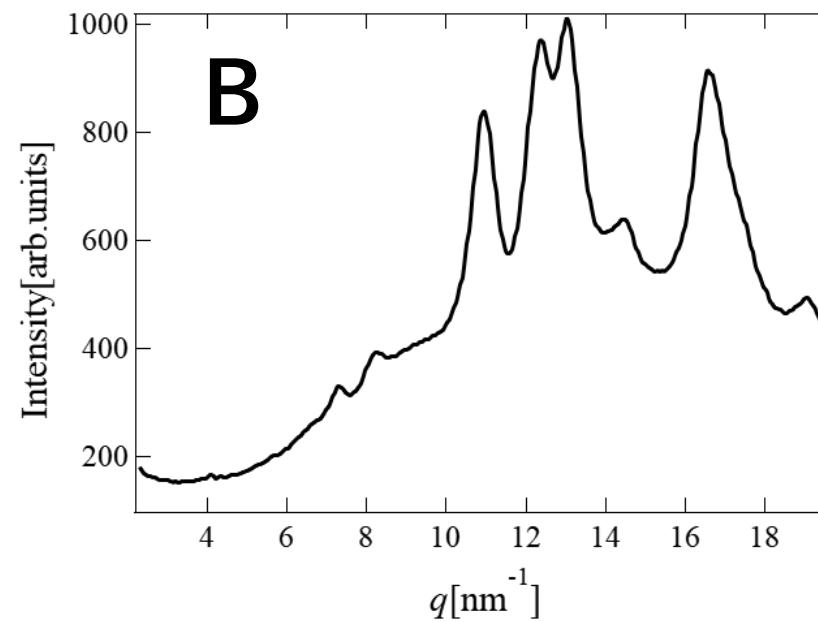
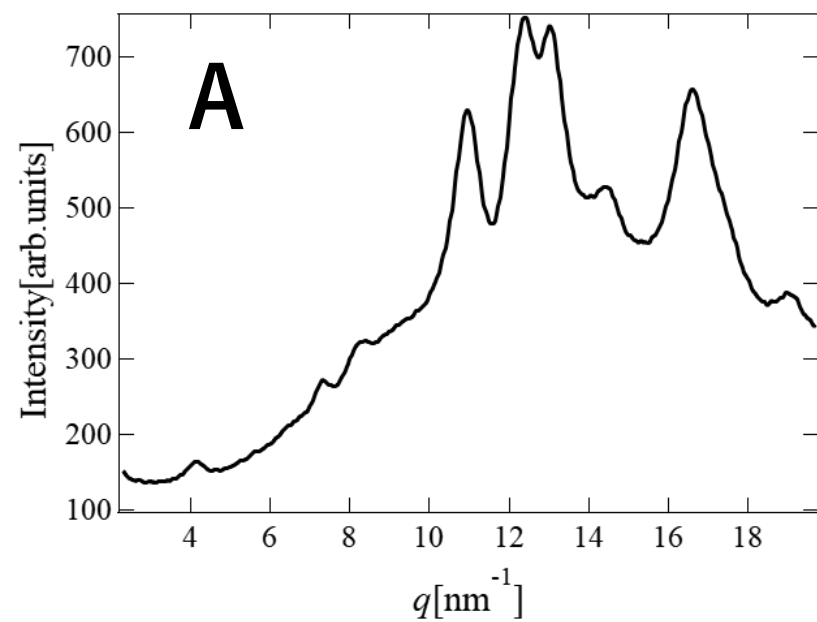


EM10



IR36ae

Fig. 6



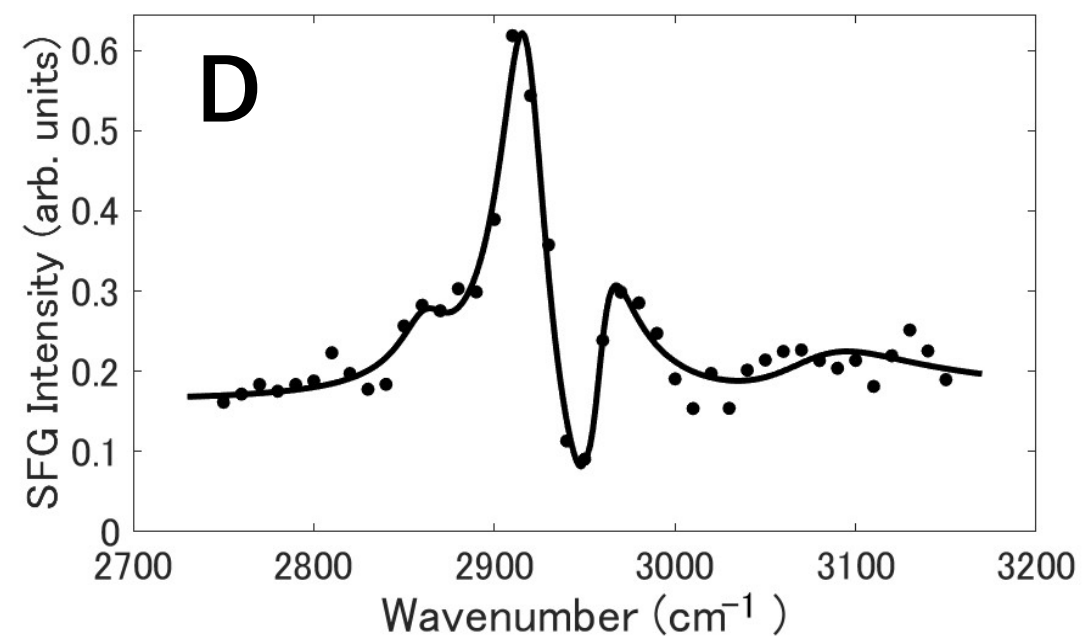
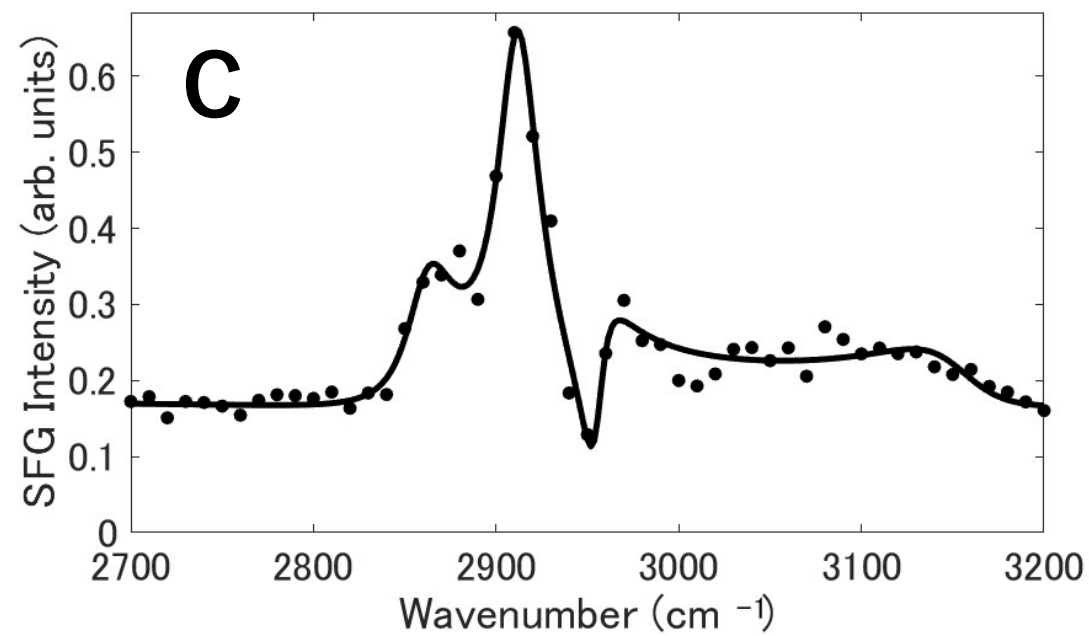
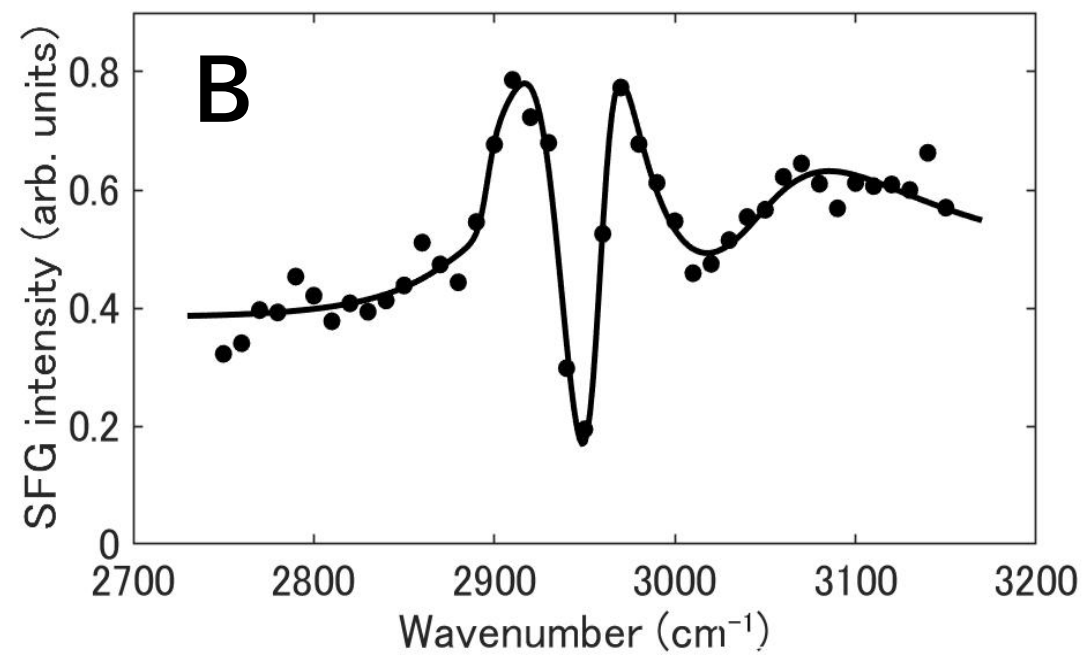
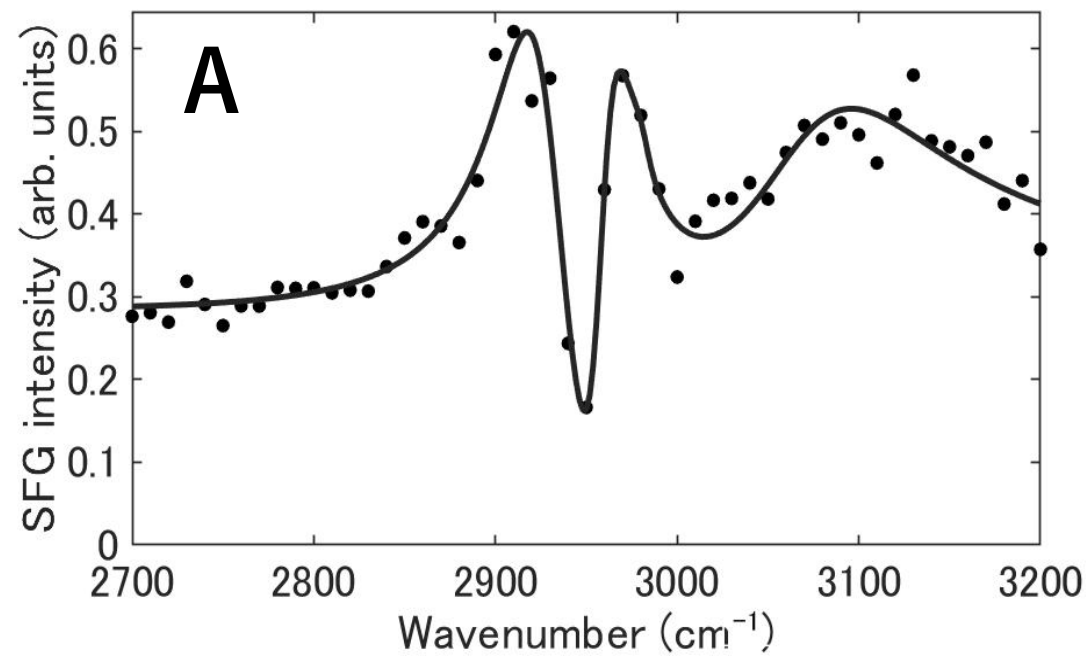


Fig. 8

